Study on the anti-coking nature of $Ni/SrTiO_3$ catalysts by the CH_4 pyrolysis

Jifei Jia [a], Eishi Tanabe [a], Peng Wang [b], Kouichi Ito [a], Hiroyuki Morioka [a], Ye Wang [c], Tetsuya Shishido [c] and Katsuomi Takehira [c,*]

[a] *Hiroshima Prefectural Institute of Industrial Science and Technology, 3-10-32 Kagamiyama, Higashi-Hiroshima 739-0046, Japan*
[b] *Japan Science and Technology Corporation, 4-1-8 Honchou, Kawaguchi 332-0012, Japan*
[c] *Department of Applied Chemistry, Graduate School of Engineering, Hiroshima University, Kagamiyama 1-4-1, Higashi-Hiroshima, Hiroshima 739-8527, Japan*
E-mail: takehira@hiroshima-u.ac.jp

Received 22 March 2001; accepted 6 July 2001

A solid phase crystallization (*spc*) method was applied for the preparation of $SrTiO_3$-supported Ni catalysts and compared to the impregnation (*imp*) method. *spc*-$Ni_{0.2}/SrTiO_3$ has highly dispersed and stable Ni metal particles resulting in higher activity and higher sustainability against coking than *imp*-$Ni_{0.2}/SrTiO_3$ in the partial oxidation of CH_4. Both catalysts were tested for the CH_4 pyrolysis in order to elucidate the catalytic nature against coking of *spc*-$Ni_{0.2}/SrTiO_3$. The amount of carbon and the rate of H_2 formation were similar over both catalysts at both 773 and 1073 K. On both catalysts, CH_4 continuously decomposed at 773 K, while the rate of CH_4 pyrolysis quickly decreased at 1073 K. Fibrous carbons grew up with a Ni metal particle on the tip of the fiber at 773 K, while carbon balls and short carbon fibers with a Ni metal particle encapsulated inside formed and no sufficient growth of the fiber was observed at 1073 K. The carbon species formed at 773 K was hydrogenated completely to CH_4 around 873 K, while the hydrogenation of that formed at 1073 K needed higher temperature around 1073 K. However, the carbon species formed on both the catalysts at either 773 or 1073 K was completely oxidized around 773 K. Thus, judging from the anti-coking nature, the behaviors in the CH_4 pyrolysis are similar over both catalysts, nonetheless *spc*-$Ni_{0.2}/SrTiO_3$ was far superior to *imp*-$Ni_{0.2}/SrTiO_3$ in the CH_4 oxidation. It is likely that the high sustainability against coking of *spc*-$Ni_{0.2}/SrTiO_3$ is not due to its intrinsic nature suppressing the coking but due to its high activity of reforming which can quickly eliminate the carbon formed on the catalyst surface.

KEY WORDS: CH_4 pyrolysis; coking; carbon nanofiber; Ni supported catalyst

1. Introduction

The catalytic conversion of CH_4 to useful chemical products has been intensively studied during the last 20 years. Recently, study has been focussed on the catalytic partial oxidation of CH_4 to synthesis gas [1–13]. This process has advantages over the conventional steam reforming of CH_4 to make synthesis gas, as the latter process is highly endothermic and produces synthesis gas having a H_2/CO ratio of 3. The partial oxidation of CH_4, expected to afford synthesis gas having the ratio of 2, makes methanol synthesis an ideal follow-up process, however, carbon deposition has been a serious problem for its industrial application [11]. It was reported that the highly dispersed metal particles on the catalyst suppressed the coke formation [14]. We have reported that perovskite-supported Ni catalysts synthesized by the "solid phase crystallization (*spc*)" method showed an excellent activity as well as enough sustainability against coke formation compared to the catalyst prepared by the impregnation (*imp*) method in the partial oxidation of CH_4 to synthesis gas [10–13]. Highly dispersed and stable Ni metal particles were formed on the surface of these catalysts, among which *spc*-$Ni_{0.2}/SrTiO_3$ showed the highest activity due to the most finely dispersed Ni metal particles. The details of the mechanism of suppressing the coke formation on these catalysts have not yet been well elucidated. Coke forms mainly by CH_4 pyrolysis or Boudouard reaction, and the former is thermodynamically preferable to the latter at the reaction temperature of 1073 K. In this paper, *spc*-$Ni/SrTiO_3$ catalyst was tested for the CH_4 pyrolysis in order to elucidate the nature of the catalyst for coke formation from CH_4 comparing to the behaviour of *imp*-$Ni/SrTiO_3$. The carbon species formed on the catalyst were investigated by SEM, TEM and temperature-programmed reactions with O_2 (TPO) and H_2 (TPH).

* To whom correspondence should be addressed.

2. Experimental

2.1. Preparation of the catalysts

Both *spc*-$Ni_{0.2}/SrTiO_3$ and *imp*-$Ni_{0.2}/SrTiO_3$ were prepared according to the previous papers [10–13]. The precursor of the *spc*-$Ni_{0.2}/SrTiO_3$ catalyst was prepared by the sol–gel method. An aqueous solution of reagent grade nickel nitrate, strontium carbonate and titanium isopropoxide was treated with an excess amount of citric acid and ethylene glycol, followed by evaporation at 353–363 K to make a

sol of organic metal complexes. This sol was decomposed by calcination at 473 K for 5 h and 773 K for 5 h, and finally calcined at 1123 K in air for 5 h. The precursor was used *in situ* for the partial oxidation of CH_4 to form Ni supported catalyst. The *imp*-$Ni_{0.2}/SrTiO_3$ catalyst was prepared as follows: the calculated amount of aqueous nickel nitrate was treated with an equimolar amount of citric acid and ethylene glycol, evaporated at 353–363 K to make a viscous liquid, and then diluted with distilled water. The solution was then added into a suspension of $SrTiO_3$ perovskite in distilled water, which was previously prepared by the sol–gel method. The suspension was again evaporated at 353–363 K, and calcined at 1123 K in air for 5 h. All the catalysts were pelletized and sieved to a size between 3.55 and 6 mm. Before catalytic testing, both *spc*-$Ni_{0.2}/SrTiO_3$ and *imp*-$Ni_{0.2}/SrTiO_3$ catalysts were examined to have perovskite structure by XRD [10–13]. Both the catalysts were *in situ* reduced during the reactions.

2.2. CH_4 oxidation over the catalysts

Each catalytic test was conducted using a fixed-bed flow reactor in a mixed gas flow of O_2, CH_4 and N_2 (20/40/80 v/v). The reaction was carried out by temperature-programmed mode under atmospheric pressure by increasing the reaction temperature from room temperature to 1073 K at the rate of 5 K min^{-1}. A reaction for testing the catalyst life was further carried out at 1073 K for 6 h under the same conditions. The activity was further compared changing the space velocity from 14000 to 112000 ml h^{-1} g-cat^{-1}. A 10 mm ∅ U-shaped quartz tube reactor was used, with the catalyst bed near the bottom. 300 mg of the catalyst was dispersed in 1.0 g of quartz sand to avoid sintering and clogging of the reactor. The thermocouple was introduced from the top of the reactor, and placed in the middle of the catalyst bed. Product gases were sampled immediately after the reactor and injected into a TCD-gas chromatograph for the analysis. Molecular Sieves 5A was used for the CO, O_2, and N_2 analyses and for the H_2 analysis with He and Ar as the carrier gas, respectively. For the analyses of air, CH_4 and CO_2, Porapak Q was used with He as the carrier gas.

After 6 h of testing the catalyst life, the reactor was filled with N_2 and then cooled down to room temperature. A temperature-programmed oxidation (TPO) experiment was performed from room temperature to 1073 K at the rate of 2.5 K min^{-1} in a mixed gas flow of N_2 and O_2 at 20 and 5 ml min^{-1}, respectively. The amount of coke formed on the catalyst was estimated from the amount of CO_2 formed during the TPO experiment.

2.3. CH_4 pyrolysis over the catalysts

Catalytic pyrolysis of CH_4 was performed in a U-shaped fixed-bed quartz reactor in a mixture of CH_4 (30 ml min^{-1}) and N_2 (30 ml min^{-1}) at 773 or 1073 K for 1 h. 100 mg of catalyst was used to test the reaction. Before the reaction, the catalyst was treated by increasing temperature from room temperature to the reaction temperature, 773 or 1073 K, at a rate of 10.0 K min^{-1} in a mixture of H_2 (8 ml min^{-1}) and N_2 (30 ml min^{-1}), and kept at the reaction temperature for 15 min. Then H_2 was swept off by N_2 (30 ml min^{-1}) at the same temperature for 20 min, and finally CH_4 (30 ml min^{-1}) was introduced. The produced gases were analyzed by on-line gas chromatography (TCD). All gases used here had a purity of 99.99%. Assuming CH_4 was completely dehydrogenated, the C/Ni atomic ratio of carbon species formed in the CH_4 pyrolysis on each catalyst was calculated by the following equation:

$$\text{C/Ni atomic ratio} = \frac{(m_{\text{total}} - m_{\text{cat}})/M_{\text{C}}}{m_{\text{cat}}\text{Wt}_{\text{Ni}}\%/M_{\text{Ni}}}, \qquad (1)$$

where m_{cat} is the initial weight of the catalyst, m_{total} is the total weight of the sample after the CH_4 pyrolysis reaction, M_{C} is the atomic weight of carbon, $\text{Wt}_{\text{Ni}}\%$ is the weight percent of Ni in the $Ni_{0.2}/SrTiO_3$ catalysts, and M_{Ni} is the atomic weight of Ni.

2.4. Characterization of carbon formed

FE-SEM (JSM-6340F) and FE-TEM (JEM-3000F 300 kV) were employed to study the carbon species formed on the catalyst in the CH_4 pyrolysis.

After the CH_4 pyrolysis, the coked catalyst was cooled to room temperature in N_2 atmosphere. Then 50 mg of the coked catalyst was used to test its reactivity to O_2 and H_2, respectively, using temperature-programmed reactions technique. The temperature was increased up to 1273 K at a rate of 2.5 K min^{-1} in a mixture of O_2 (5 ml min^{-1}) and N_2 (20 ml min^{-1}) for TPO, or H_2 (30 min^{-1}) and N_2 (20 ml min^{-1}) for TPH, respectively. The analysis of the products was as the same as the analysis in the CH_4 pyrolysis. All gases used here were with a purity of 99.99%.

3. Results and discussion

3.1. CH_4 oxidation over spc-$Ni_{0.2}/SrTiO_3$ and imp-$Ni_{0.2}/SrTiO_3$

The reaction was carried out with the feed gas of stoichiometric composition ($CH_4/O_2 = 2$ with N_2), at GHSV = 14000 ml h^{-1} g-cat^{-1} over *spc*-$Ni_{0.2}/SrTiO_3$ and *imp*-$Ni_{0.2}/SrTiO_3$. The results are shown in figure 1. It is clearly seen that CH_4 began to react with O_2 at 773 K to form CO_2 and H_2O by the combustion (1) around 950 K,

$$CH_4 + 2O_2 \rightleftharpoons CO_2 + 2H_2O \qquad (1)$$

followed by reforming of CH_4 with H_2O or CO_2 to form synthesis gas CO/H_2 ((2) and (3)) at 1073 K,

$$CH_4 + H_2O \rightleftharpoons CO + 3H_2 \qquad (2)$$

$$CH_4 + CO_2 \rightleftharpoons 2CO + 2H_2 \qquad (3)$$

Thus CH_4 conversion reached to the value controlled by thermodynamic equilibrium of the reformings. *spc*-$Ni_{0.2}$/

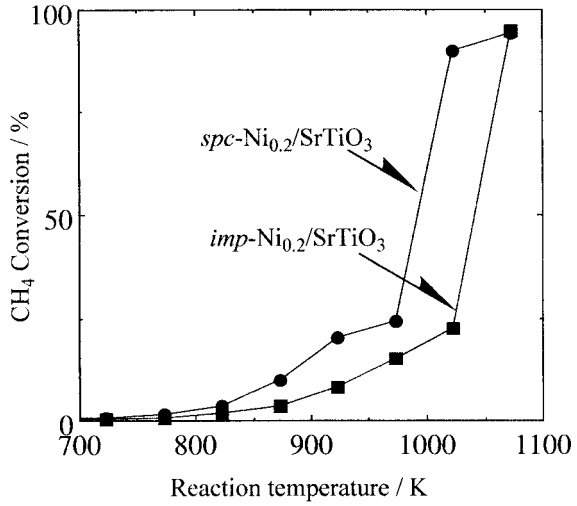

Figure 1. CH_4 oxidation at 1073 K over *spc*-$Ni_{0.2}/SrTiO_3$ and *imp*-$Ni_{0.2}/SrTiO_3$.

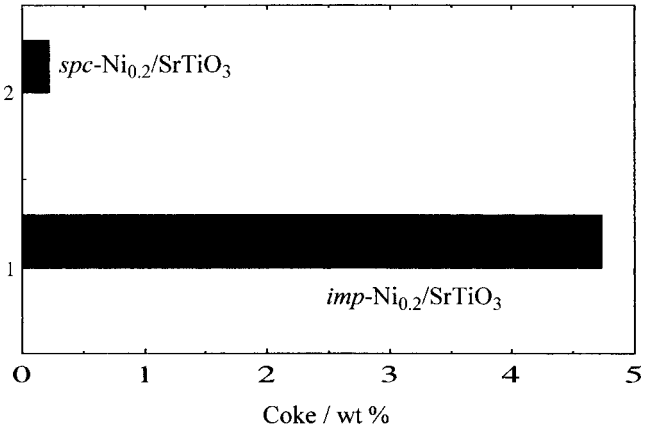

Figure 2. Amount of coke deposited on *spc*-$Ni_{0.2}/SrTiO_3$ and *imp*-$Ni_{0.2}/SrTiO_3$ after the CH_4 oxidation for 6 h.

$SrTiO_3$ showed higher activity than *imp*-$Ni_{0.2}/SrTiO_3$. As previously reported in the analytical results with XRD and TEM [13], finely dispersed Ni metal particles were more intensively observed over *spc*-$Ni_{0.2}/SrTiO_3$ than over *imp*-$Ni_{0.2}/SrTiO_3$ after the reaction. The amount of coke deposited on the catalyst after the reaction for 6 h was measured and shown in figure 2. A clear difference was observed in the coke amount between *spc*-$Ni_{0.2}/SrTiO_3$ and *imp*-$Ni_{0.2}/SrTiO_3$, and over 20 times more amount of coke was detected over the latter compared to over the former. This may be uniquely due to the presence of a larger size of Ni metal particles on *imp*-$Ni_{0.2}/SrTiO_3$ compared to *spc*-$Ni_{0.2}/SrTiO_3$.

Under the condition of GHSV = 14000 ml h^{-1} g-cat^{-1}, no significant difference was observed in the activity between *spc*-$Ni_{0.2}/SrTiO_3$ and *imp*-$Ni_{0.2}/SrTiO_3$. It is likely that thermodynamic equilibrium of the reactions (1)–(3) was attained over these catalysts under the conditions of low GHSV. The activity was further tested at increasing space velocity (figure 3). At the higher space velocity, the catalytic activity can be compared more precisely, since the

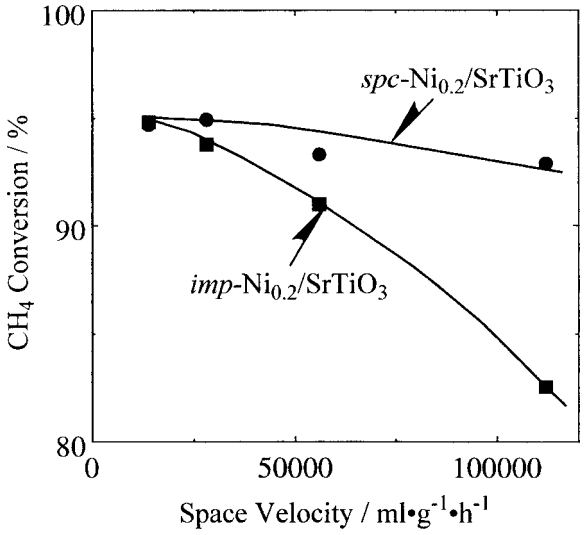

Figure 3. Effect of the space velocity in the CH_4 oxidation over *spc*-$Ni_{0.2}/SrTiO_3$ and *imp*-$Ni_{0.2}/SrTiO_3$.

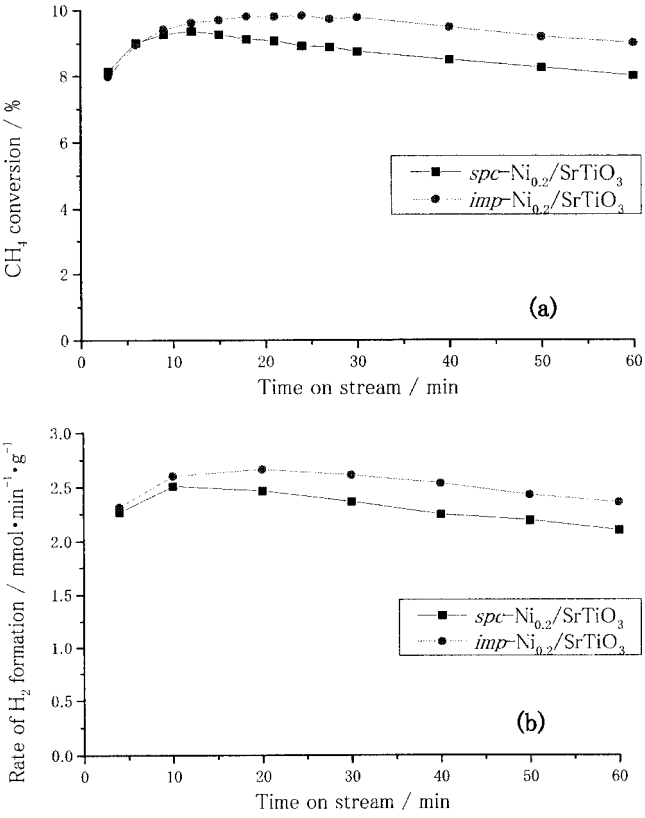

Figure 4. CH_4 pyrolysis at 773 K for 1 h on *spc*-$Ni_{0.2}/SrTiO_3$ and *imp*-$Ni_{0.2}/SrTiO_3$. (a) CH_4 conversion *vs.* reaction time. (b) Rate of H_2 formation *vs.* reaction time.

reaction might be controlled kinetically. Even at the high space velocity of 112000 ml h^{-1} g-cat^{-1}, the activity of *spc*-$Ni_{0.2}/SrTiO_3$ was still high enough, while the activity of *imp*-$Ni_{0.2}/SrTiO_3$ substantially decreased. *spc*-$Ni_{0.2}/SrTiO_3$ may *in situ* release nickel species from the structure to the surface during the reaction, followed by the formation of the highly dispersed Ni species.

Table 1
C/Ni atomic ratio of carbon species formed in CH_4 pyrolysis on *spc*-$Ni_{0.2}/SrTiO_3$ and *imp*-$Ni_{0.2}/SrTiO_3$ at 773 and 1073 K for 1 h.

Catalyst	Reaction temperature (K)	C/Ni atomic ratio
spc-$Ni_{0.2}/SrTiO_3$	773	56
imp-$Ni_{0.2}/SrTiO_3$	773	62
spc-$Ni_{0.2}/SrTiO_3$	1073	7
imp-$Ni_{0.2}/SrTiO_3$	1073	12

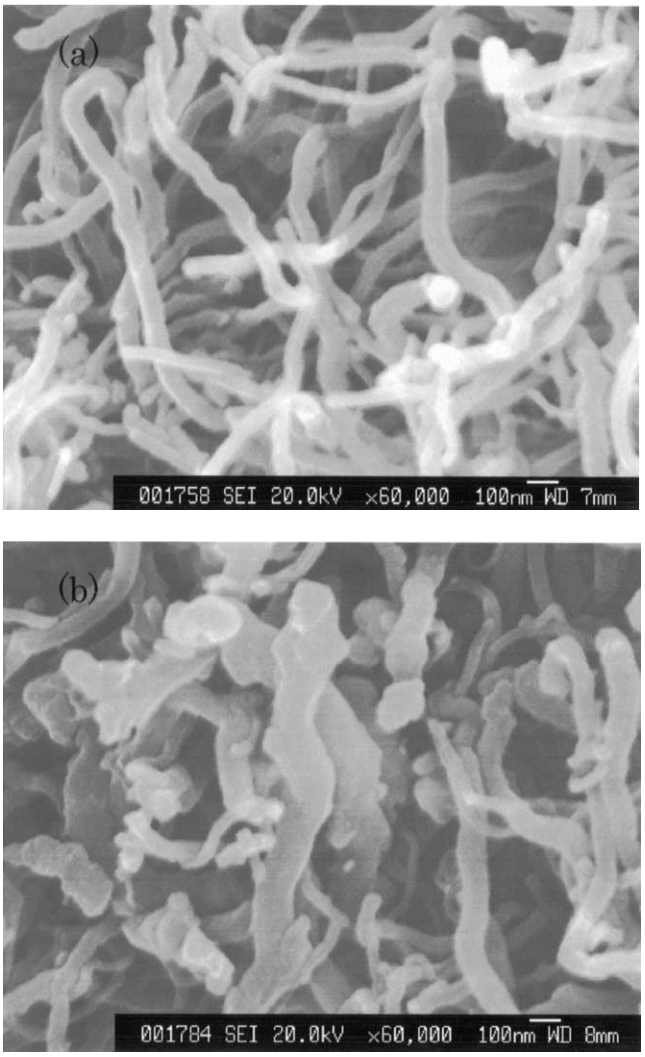

Figure 5. SEM images of the carbon species formed in CH_4 pyrolysis at 773 K for 1 h on (a) *spc*-$Ni_{0.2}/SrTiO_3$ and (b) *imp*-$Ni_{0.2}/SrTiO_3$.

3.2. CH_4 pyrolysis on spc-$Ni_{0.2}/SrTiO_3$ and imp-$Ni_{0.2}/SrTiO_3$ at 773 K

Figure 4 shows the CH_4 pyrolysis at 773 K for 1 h on *spc*-$Ni_{0.2}/SrTiO_3$ and *imp*-$Ni_{0.2}/SrTiO_3$. The CH_4 conversion and the rate of H_2 formation on *imp*-$Ni_{0.2}/SrTiO_3$ were slightly higher than those on *spc*-$Ni_{0.2}/SrTiO_3$. During the reactions, only CH_4 and H_2 were detected in the gas phase. Assuming CH_4 was completely dehydrogenated, the molar ratio between the carbon species and H_2 formed on both the catalysts was about 0.5 (integration of the rate of H_2 formation gave the total amount of H_2). Therefore the formed carbon species contained negligible amount of hydrogen. The C/Ni atomic ratio of the carbon species formed in the CH_4 pyrolysis on both catalysts for 1 h was determined (table 1). The C/Ni ratio on *imp*-$Ni_{0.2}/SrTiO_3$ was slightly higher than that on *spc*-$Ni_{0.2}/SrTiO_3$.

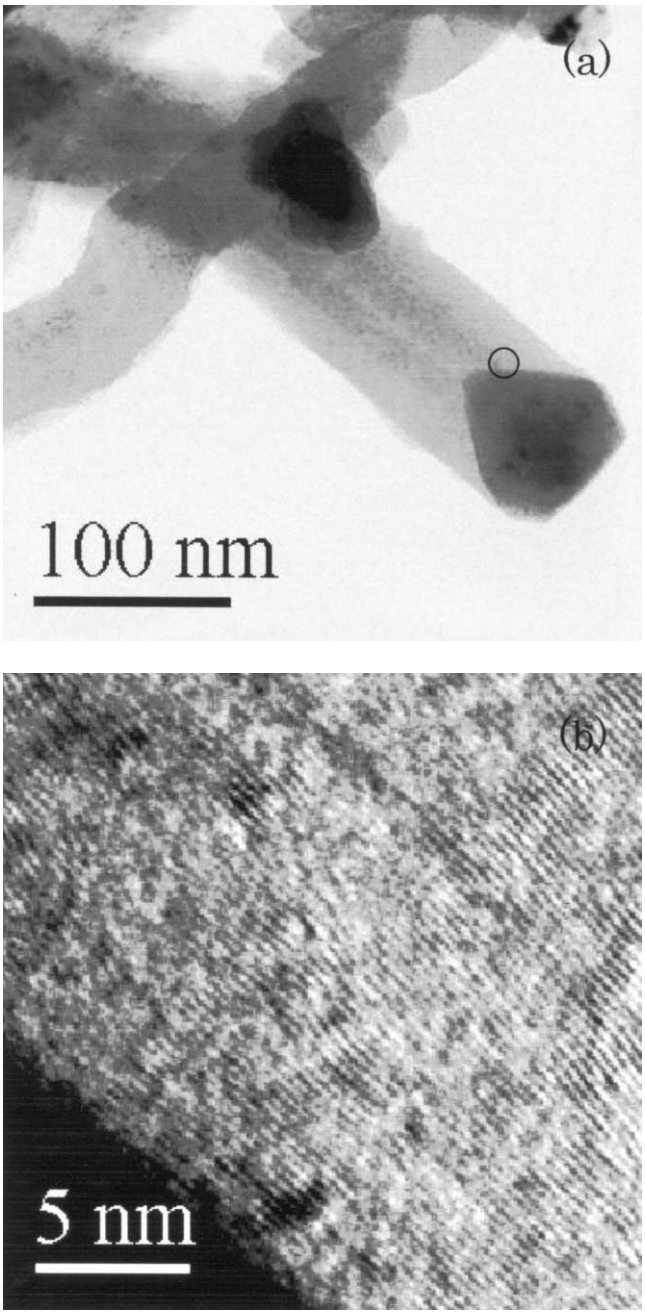

Figure 6. (a) TEM micrograph and (b) high-resolution micrograph of the carbon species formed in CH_4 pyrolysis at 773 K for 1 h on *spc*-$Ni_{0.2}/SrTiO_3$.

SEM images of the carbon species formed in the CH_4 pyrolysis at 773 K for 1 h on both catalysts are shown in figure 5. From the SEM images, it is known that carbon species formed on both the catalysts were all in fiber shape which demonstrated that a filamentous carbon growth oc-

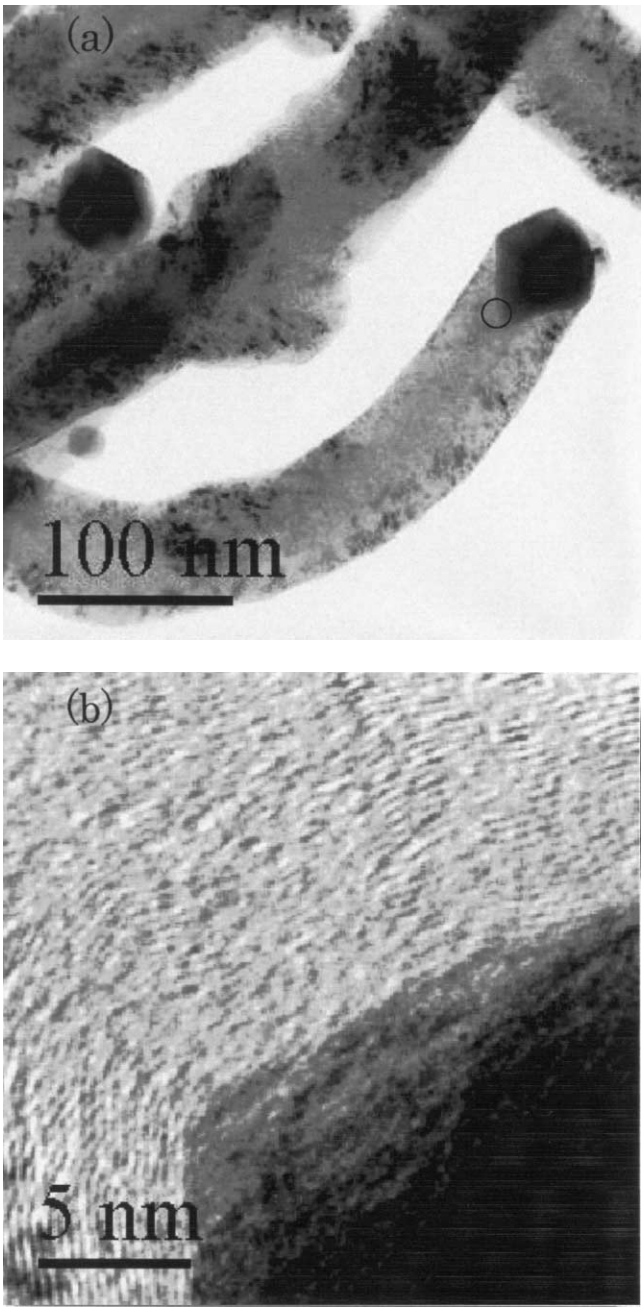

Figure 7. (a) TEM micrograph and (b) high-resolution micrograph of the carbon species formed in CH_4 pyrolysis at 773 K for 1 h on *imp*-$Ni_{0.2}/SrTiO_3$.

curred on the catalysts. The distribution of outer diameters of the carbon fibers formed in the CH_4 pyrolysis on *spc*-$Ni_{0.2}/SrTiO_3$ (20–90 nm) was narrower than that on *imp*-$Ni_{0.2}/SrTiO_3$ (20–140 nm).

The structures of the carbon fibers were also studied by TEM (figures 6 and 7). The carbon fibers formed on the catalysts were solid fibers (figures 6(a) and 7(a)) composed of graphite platelets which stacked on the Ni metal particle (figures 6(b) and 7(b)). The distance between the platelets, obtained from figure 6(b), was about 0.34 nm. A Ni metal particle anchored on the tip of a solid carbon fiber and, therefore, a carbon "tip-growth" mechanism played a key role in

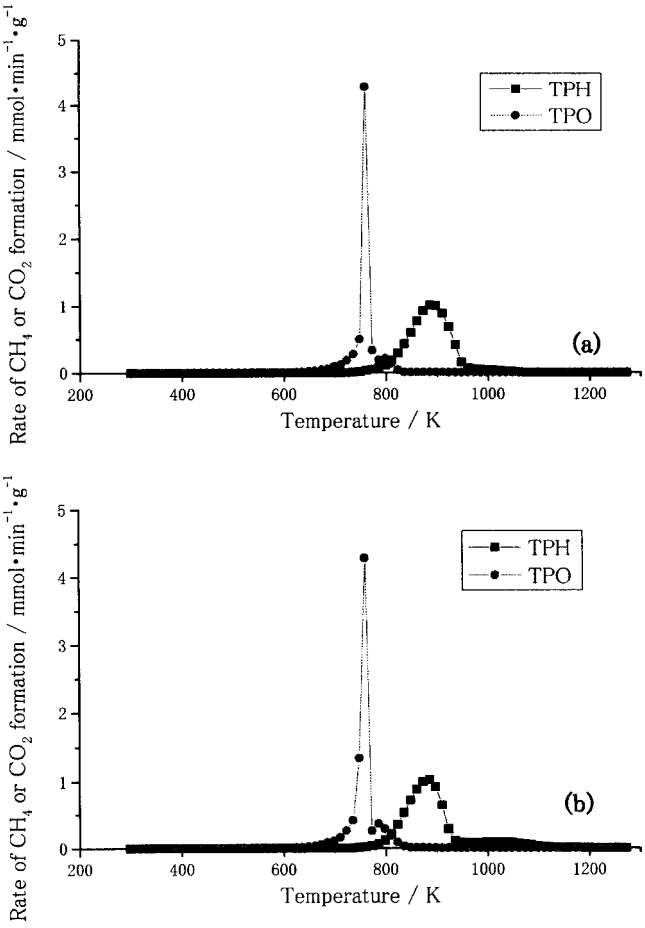

Figure 8. TPO and TPH profiles of the carbon species formed in CH_4 pyrolysis at 773 K for 1 h on (a) *spc*-$Ni_{0.2}/SrTiO_3$ and (b) *imp*-$Ni_{0.2}/SrTiO_3$.

the CH_4 pyrolysis [15]. Because the metal particle size determined the size of carbon fiber in the carbon "tip-growth" mechanism, *imp*-$Ni_{0.2}/SrTiO_3$ is considered to have broader Ni metal particle sizes distribution than *spc*-$Ni_{0.2}/SrTiO_3$. This well agreed with the results obtained in the SEM images.

TPO and TPH of the carbon species formed in the CH_4 pyrolysis on both catalysts at 773 K were conducted to study carbon species' reactivity toward O_2 and H_2. TPO and TPH profiles of carbon species formed in the CH_4 pyrolysis at 773 K for 1 h on *spc*-$Ni_{0.2}SrTiO_3$ are shown in figure 8(a). During the TPO process, the CO_2 signal was observed between 523 and 923 K. A main peak with its maximum rate of CO_2 formation at 763 K and a small peak with its maximum rate of CO_2 formation at 798 K were observed in the process. CO_2 alone was observed as the product in the TPO process. The amount of the carbon species measured on the coked *spc*-$Ni_{0.2}/SrTiO_3$ before TPO well coincided with that calculated from CO_2 formed in the TPO process, suggesting that carbon species was oxidized completely under the present TPO condition. From the TPO profile, it is likely that there were two kinds of carbon species on the *spc*-$Ni_{0.2}/SrTiO_3$ surface. The main peak at 763 K can be assigned to solid carbon fibers formed on the Ni metal particles. The small peak

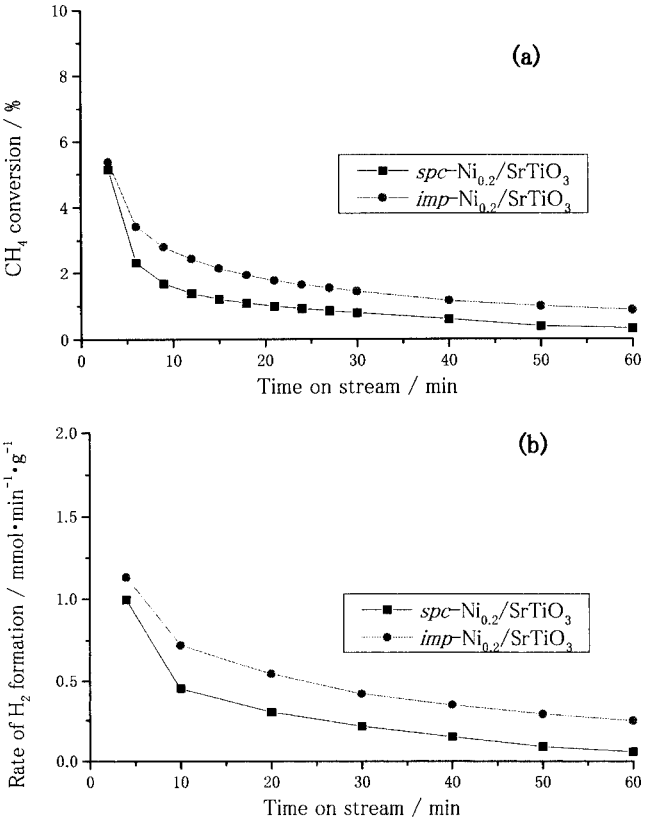

Figure 9. CH_4 pyrolysis at 1073 K for 1 h on *spc*-$Ni_{0.2}/SrTiO_3$ and *imp*-$Ni_{0.2}/SrTiO_3$. (a) CH_4 conversion *vs.* reaction time and (b) rate of H_2 formation *vs.* reaction time.

at 798 K can be assigned to the carbon species on the $SrTiO_3$ support, which probably formed by the CH_4 pyrolysis on the $SrTiO_3$ support directly or by overgrowing from the Ni metal particles [16]. Because of its small amount, the carbon species on $SrTiO_3$ was hardly observed by TEM. During the TPH process, the CH_4 signal was observed between 723 and 1073 K. A main peak with its maximum rate of CH_4 formation at 883 K and a long tail up to 1073 K were observed in the process. No higher hydrocarbon was detected in the TPH process. The carbon species was hydrogenated completely in the TPH process too. Accordingly, the main peak in the TPH process can be assigned to solid carbon fibers formed on the Ni metal particles, while the long tail to the carbon species on the $SrTiO_3$ support. Comparison between the TPO and TPH profiles indicates that the carbon species formed on *spc*-$Ni_{0.2}/SrTiO_3$ was more reactive to O_2.

TPO and TPH of the carbon species formed in the CH_4 pyrolysis at 773 K for 1 h over *imp*-$Ni_{0.2}/SrTiO_3$ (figure 8(b)) gave similar results to those on *spc*-$Ni_{0.2}/SrTiO_3$. In the TPO process, the main peak was found in the same position as that on *spc*-$Ni_{0.2}/SrTiO_3$, but the small peak was found with its maximum rate of CO_2 formation at 788 K. In the TPH process, the main peak was found in same position as that on *spc*-$Ni_{0.2}/SrTiO_3$ but the long tail ended at 1198 K. The carbon species were completely removed by O_2 and H_2 during the TPO and TPH processes.

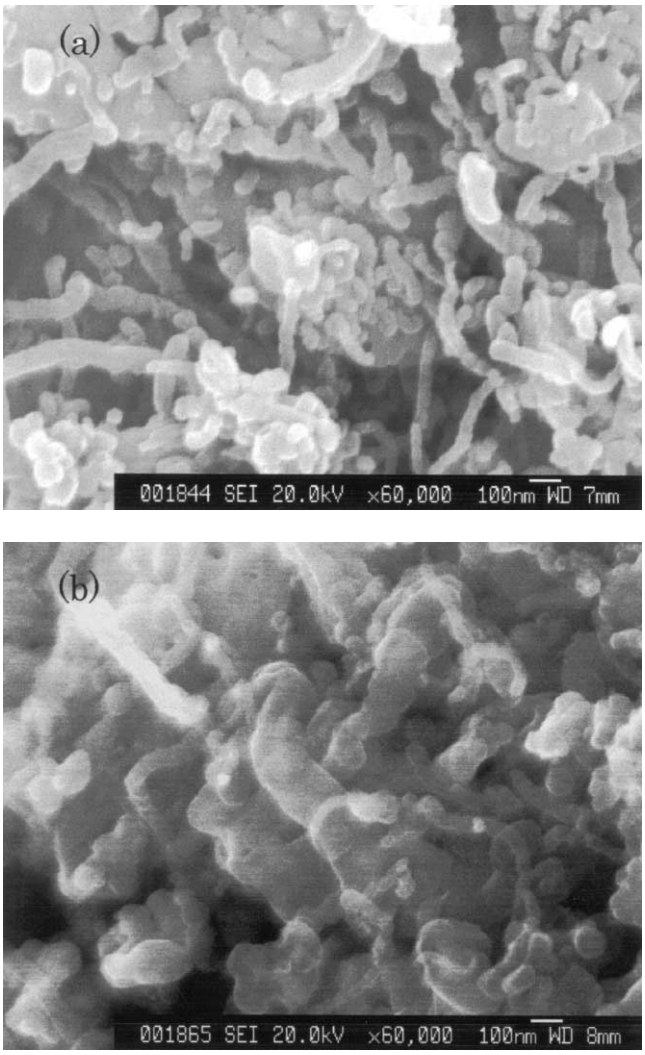

Figure 10. SEM images of the carbon species formed in CH_4 pyrolysis at 1073 K for 1 h on (a) *spc*-$Ni_{0.2}/SrTiO_3$ and (b) *imp*-$Ni_{0.2}/SrTiO_3$.

3.3. CH_4 pyrolysis on spc-$Ni_{0.2}/SrTiO_3$ and imp-$Ni_{0.2}/SrTiO_3$ at 1073 K

CH_4 was pyrolysed on *spc*-$Ni_{0.2}/SrTiO_3$ and *imp*-$Ni_{0.2}/SrTiO_3$ at 1073 K for 1 h (figure 9). Similarly to the results at 773 K, the CH_4 conversion and the rate of H_2 production on *imp*-$Ni_{0.2}/SrTiO_3$ were slightly higher than those on *spc*-$Ni_{0.2}/SrTiO_3$. Also, only CH_4 and H_2 were detected in the gas phase during the reactions. The C/Ni ratio of the carbon species formed at 1073 K on *imp*-$Ni_{0.2}/SrTiO_3$ was slightly higher than that on *spc*-$Ni_{0.2}/SrTiO_3$ (table 1). However the C/Ni ratio of those formed at 1073 K on both the catalysts were far lower than those formed at 773 K. The amount of the carbon species was also approximately 0.5 times the amount of H_2 formed in the CH_4 pyrolysis on both the catalysts.

SEM images of the carbon species formed in the CH_4 pyrolysis at 1073 K on both catalysts are shown in figure 10. On both the catalysts, carbon deposited in fiber shape or sometimes in ball shape, and the length of fiber was much shorter than those formed at 773 K. The distribution of outer

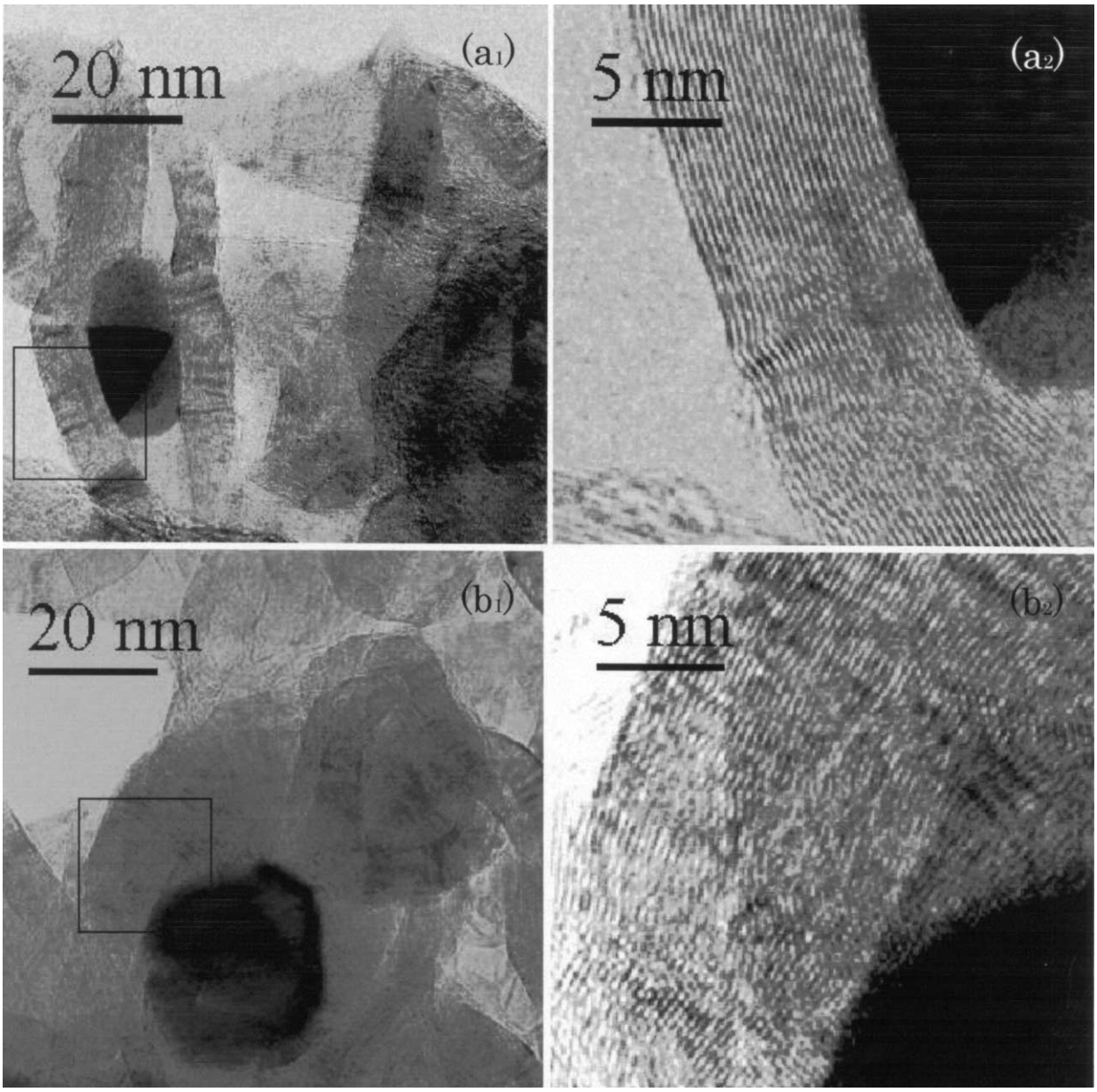

Figure 11. (a_1) TEM micrograph, (a_2) high-resolution micrograph of carbon fiber and (b_1) TEM micrograph, (b_2) high-resolution micrograph of carbon ball formed in CH_4 pyrolysis at 1073 K for 1 h on *spc*-$Ni_{0.2}/SrTiO_3$.

diameters of the carbon fibers formed at 1073 K on *spc*-$Ni_{0.2}/SrTiO_3$ (20–90 nm) was also narrower than that on *imp*-$Ni_{0.2}/SrTiO_3$ (20–160 nm).

TEM images of the carbon species formed on *spc*-$Ni_{0.2}/SrTiO_3$ at 1073K for 1 h (figure 11) indicate that, similar to the SEM observations, there were two kinds of carbon species on the catalyst surface. One kind of carbon was hollow graphitic fibers (figure 11 (a_1) and (a_2)) and a Ni metal particle was located in a hollow nano-fiber, with the same width as the inner diameter of the hollow fiber. Therefore, the inner diameter of the carbon fiber depended on the Ni metal particle size. It is suggested, in this case, that the fibers were formed *via* a bi-directional precipitation of carbon on the opposite faces on the Ni metal particles [17]. The other kind of carbon, which covered a Ni metal particle (figure 11 (b_1) and (b_2)), consisted of graphitic platelets oriented parallel to the Ni metal particle. It corresponds to the carbon ball observed by SEM.

TEM images of the carbon species formed in the CH_4 pyrolysis on *imp*-$Ni_{0.2}/SrTiO_3$ at 1073 K for 1 h are shown in figure 12. Two kinds of carbon species were observed in this case too. One was solid graphitic carbon fibers (figure 12 (a_1) and (a_2)) in which Ni metal particles located and the other was a graphitic carbon ball with a Ni metal particle inside (figure 12 (b_1) and (b_2)).

TPO and TPH of the carbon species formed in the CH_4 pyrolysis at 1073 K for 1 h on *spc*-$Ni_{0.2}/SrTiO_3$ are shown in figure 13(a). During the TPO process CO_2 was observed between 523 and 923 K as the only product. A peak with its maximum rate of CO_2 formation at 763 K was observed

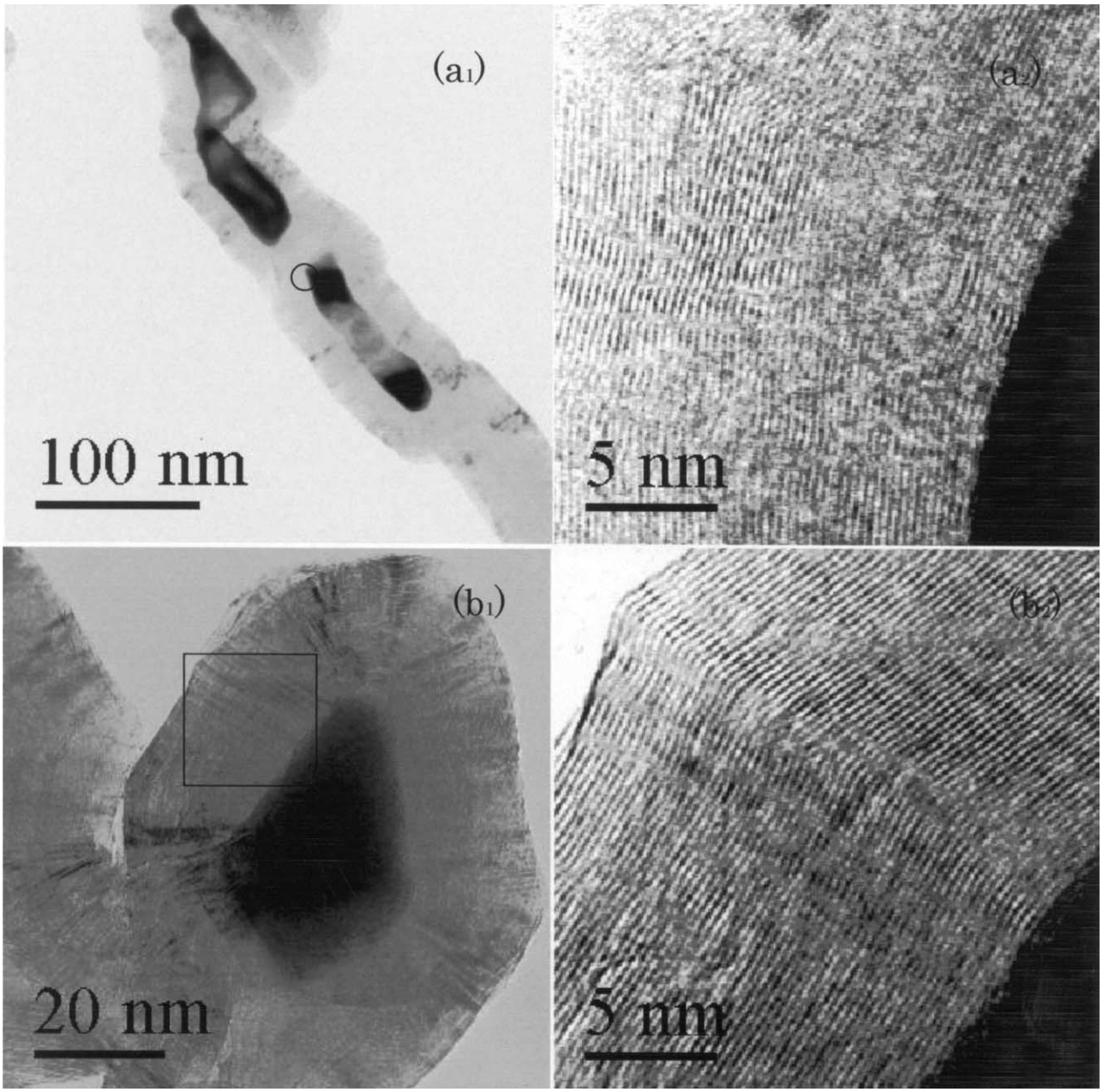

Figure 12. (a_1) TEM micrograph, (a_2) high-resolution micrograph of carbon fiber and (b_1) TEM micrograph, (b_2) high-resolution micrograph of carbon ball formed in CH_4 pyrolysis at 1073 K for 1 h on *imp*-$Ni_{0.2}/SrTiO_3$.

in the process. The peak was assigned to oxidation of the carbon fibers and carbon balls formed on the Ni metal particles. No peak responsible to carbon species on the $SrTiO_3$ support was found. The carbon species formed at 1073 K on *spc*-$Ni_{0.2}/SrTiO_3$ had been oxidized completely under the present TPO condition. During the TPH process, CH_4 was observed between 923 and 1273 K as the only product. A broad peak with its maximum rate of CH_4 formation at 1023 K and a long tail up to 1273 K were observed. Even at 1273 K, unhydrogenated carbon species still remained (15 wt% of the carbon species remained after the TPH process). Therefore, the carbon species formed on Ni metal particles at 1273 K could not be hydrogenated completely under the present TPH condition.

TPO and TPH of carbon species formed in CH_4 decomposition at 1073 K for 1 h on *imp*-$Ni_{0.2}/SrTiO_3$ (figure 13(b)) were similar to the results on *spc*-$Ni_{0.2}/SrTiO_3$. The carbon species formed at 1073 K on *imp*-$Ni_{0.2}/SrTiO_3$ had been oxidized completely under the TPO condition but 10 wt% of the carbon species remained after the TPH process.

It is clear that the amount of carbon species formed in the CH_4 pyrolysis on *imp*-$Ni_{0.2}/SrTiO_3$ was slightly greater than that over *spc*-$Ni_{0.2}/SrTiO_3$ at both 773 and 1073 K. This is attributed to the *spc* method giving the higher dispersion of Ni metal particles on the $SrTiO_3$ support [10–13]. It is interesting to note that the amount of carbon species formed at 1073 K on both the catalysts was much smaller than the amount of carbon species formed at 773 K. Thermodynamic

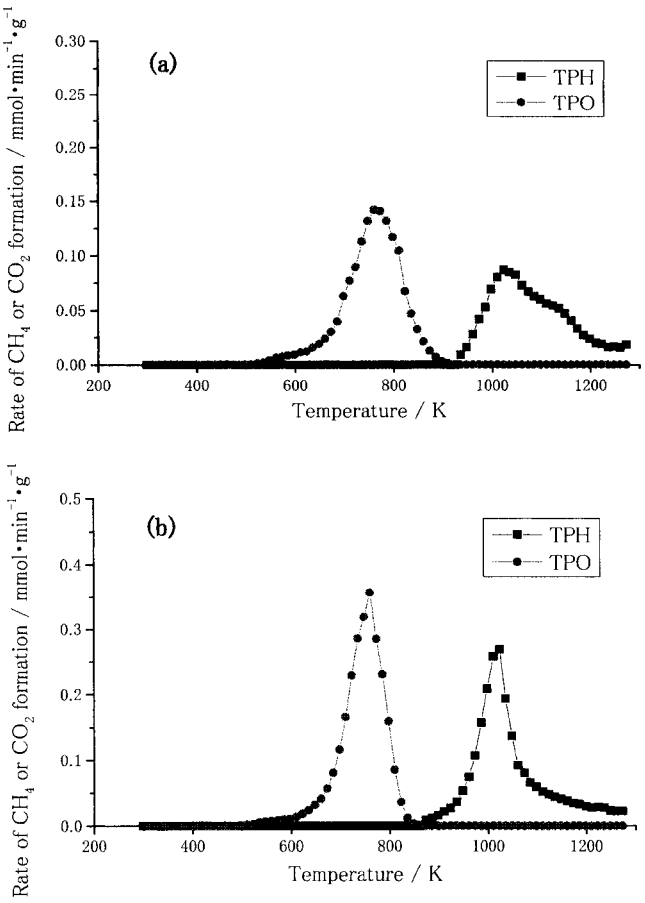

Figure 13. TPO and TPH profiles of the carbon species formed in CH_4 pyrolysis at 1073 K for 1 h on (a) *spc*-$Ni_{0.2}/SrTiO_3$ and (b) *imp*-$Ni_{0.2}/SrTiO_3$.

calculation indicates that CH_4 is more easily decomposed at 1073 K than at 773 K [18]. Therefore, it is likely that a quick deactivation by coke formation occurred in the CH_4 pyrolysis on both catalysts at 1073 K. The smaller amount of carbon species formed at 1073 K than at 773 K might be explained as follows: at 1073 K, Ni particles, which were encapsulated inside by coke, could not play a catalytic role for CH_4 pyrolysis, whereas at 773 K, Ni particles, which were on the tip of the carbon fiber, kept their catalytic activity. The carbon species formed in the CH_4 pyrolysis on both the catalysts at 1073 K showed almost the same reactivity to O_2 as those formed at 773 K. However, the carbon species formed on both catalysts at 773 K were more reactive to H_2 than those formed at 1073 K. The carbon species formed on both catalysts reacted with O_2 at the lower temperature around 773 K than with H_2, suggesting that the carbon could be easily removed by O_2 during the partial oxidation of CH_4 at 1073 K.

It was previously reported that the *spc*-$Ni_{0.2}/SrTiO_3$ catalyst showed high activity as well as high sustainability against coke formation during the partial oxidation of CH_4 at 1073 K, as shown in figures 1–3 [13]. This is due to the highly dispersed and stable Ni metals particles on *spc*-$Ni_{0.2}/SrTiO_3$. C/Ni atomic ratio calculated from the results of figure 2 is 0.18 and 3.84 for *spc*-$Ni_{0.2}/SrTiO_3$ and *imp*-$Ni_{0.2}/SrTiO_3$, respectively, after the CH_4 oxidation at 1073 K for 6 h. These values seem too small compared to those obtained in the CH_4 pyrolysis for 1 h (table 1) considering the reaction time. More than 20 times larger amount of carbon deposited in the CH_4 oxidation, while less than 2 times larger amount of carbon was observed in the CH_4 pyrolysis, on *spc*-$Ni_{0.2}/SrTiO_3$ compared to *imp*-$Ni_{0.2}/SrTiO_3$. Moreover, the CH_4 oxidation was not significantly retarded over the catalysts. However, in the CH_4 pyrolysis, both catalysts were quickly deactivated by coke formation and no significant difference was observed between *spc*-$Ni_{0.2}/SrTiO_3$ and *imp*-$Ni_{0.2}/SrTiO_3$ in the sustainability against coking (table 1). The CH_4 pyrolysis is more appropriate than the CO disproportionation as an origin of the coke formation at 1073 K. It is therefore clear that high dispersion of Ni metal particles alone is not sufficient for protecting the catalyst from coke formation. Coke must be eliminated by the succeeding reforming reactions. It is likely that high activity of the reforming reaction is important for affording the high sustainability against coking on the catalyst.

4. Conclusion

The carbon formation was studied in the CH_4 pyrolysis over *spc*-$Ni_{0.2}/SrTiO_3$ and *imp*-$Ni_{0.2}/SrTiO_3$ at 773 and 1073 K and discussed on related to the anti-coking nature of *spc*-$Ni_{0.2}/SrTiO_3$ in the CH_4 oxidation at 1073 K. In the CH_4 oxidation, *spc*-$Ni_{0.2}/SrTiO_3$ showed clearly higher activity as well as higher sustainability against coking than *imp*-$Ni_{0.2}/SrTiO_3$. In the CH_4 pyrolysis, graphitic carbon fibers formed on both the catalysts and a Ni metal particle anchored on the tip of the fiber at 773 K, while ball-shaped carbon with a Ni metal particle inside was observed over both catalysts at 1073 K. The C/Ni atomic ratio was significantly higher in the CH_4 oxidation, but almost similar in the CH_4 pyrolysis, on *imp*-$Ni_{0.2}/SrTiO_3$ compared to *spc*-$Ni_{0.2}/SrTiO_3$ at 1073 K. The carbon species formed in the CH_4 pyrolysis on both catalysts at 1073 K were rather reactive to O_2. Thus no significant difference was observed between *spc*-$Ni_{0.2}/SrTiO_3$ and *imp*-$Ni_{0.2}/SrTiO_3$ from the view point of anti-coking nature in the CH_4 pyrolysis. On both catalysts at 773 K, CH_4 was pyrolysed to form carbon atoms on the surface of Ni metal particles, which migrated to the site where filamentous carbon growth occurred steadily. At 1073 K, CH_4 was quickly pyrolysed to form numerous carbon atoms that in turn quickly covered all the surface of Ni metal particles, resulting in the deactivation of both the catalysts. It is thus likely that the high sustainability against coking of the *spc*-$Ni_{0.2}/SrTiO_3$ catalyst is not due to its intrinsic nature suppressing the coking but due to its high activity of reforming which can quickly eliminate the carbon formed on the catalyst surface.

References

[1] A.T. Ashcroft, A.K. Cheetham, J.S. Foord, M.L.H. Green, C.P. Grey, A.J. Murrell and P.D. Vernon, Nature 344 (1990) 319.
[2] D. Dissanayake, M.P. Rosynek, K.C.C. Kharas and J.H. Lunsford, J. Catal. 132 (1991) 117.
[3] D.A. Hickman and L.D. Schmidt, Science 295 (1993) 343.
[4] V.R. Chaudhary, A.M. Rajput and V.H. Rane, J. Phys. Chem. 96 (1992) 8686.
[5] E. Ruckenstein and H.Y. Wang, J. Catal. 187 (1999) 151.
[6] Y.H. Hu and E. Ruckenstein, J. Catal. 158 (1996) 260.
[7] Y. Xu and L. Lin, Appl. Catal. A 188 (1999) 53.
[8] S.C. Tsang, J.B. Claridge and M.L.H. Green, Catal. Today 23 (1996) 3.
[9] N. Matsui, K. Nakagawa, N. Ikenaga and T. Suzuki, J. Catal. 194 (2000) 115.
[10] T. Hayakawa, H. Harihara, A.G. Andersen, A.P.E. York, K. Suzuki, H. Yasuda and K. Takehira, Angew. Chem. Int. Ed. Engl. 35 (1996) 192.
[11] T. Hayakawa, H. Harihara, A.G. Andersen, K. Suzuki, H. Yasuda, T. Tsunoda, S. Hamakawa, A.P.E. York, Y.S. Yoon, M. Shimizu and K. Takehira, Appl. Catal. A 149 (1997) 391.
[12] R. Shiozaki, A.G. Anderson, T. Hayakawa, S. Hamakawa, K. Suzuki, M. Shimizu and K. Takehira, J. Chem. Soc. Faraday Trans. 93 (1997) 3235.
[13] K. Takehira, T. Shishido and M. Kondo, Shokubai 42 (2000) 354.
[14] C.H. Bartholomew, Catal. Rev. Sci. Eng. 24 (1982) 67.
[15] S.B. Sinnott, R. Andrews, D. Qian, A.M. Rao, Z. Mao, E.C. Dickey and F. Derbyshire, Chem. Phys. Lett. 315 (1999) 25.
[16] J.H. Bitter, K. Seshan and J.A. Lercher, J. Catal. 183 (1999) 336.
[17] Y.H. Hu and E. Ruckenstein, J. Catal. 184 (1999) 298.
[18] J.B. Claridge, M.L.H. Green, S.C. Tsang, A.P.E. York, A.T. Ashcroft and P.D. Battle, Catal. Lett. 22 (1993) 299.